Energetic Isomers of 1,2,4,5-Tetrazine-bis-1,2,4-Triazoles with Low Toxicity

Supporting Information

A. Shlomovich,[a] T. Pechersky,[a] A. Cohen,[a] Q. L. Yan,*[b] M. Kosa,[c] N. Petrutik,[a] N. Tal,[a] A. Aizikovich,*[a] and M. Gozin*[a]

[a] School of Chemistry, Faculty of Exact Sciences, Tel-Aviv University, Tel-Aviv 69978, Israel.
[b] Science and Technology on Combustion, Internal Flow and Thermal-structure Laboratory, Northwestern Polytechnical University, Xi'an 710072, China.
[c] Schulich Faculty of Chemistry, Technion - Israel Institute of Technology, Haifa 32000, Israel.

X-ray Crystallography

Crystals of compound **5** suitable for x-ray diffraction were obtained by subjecting a solution of **5** in DMSO to vapors of Ethyl acetate. Data was collected using MoKa radiation (L = 0.71073 nm). An Oxford low-temperature device was used to keep the crystals at a constant temperature of 110K, during all data collection period. Details of the x-ray data collection and structure refinements are summarized in Table S1. CCDC 1445126 contain the supplementary crystallographic data for this paper. These data can be obtained free of charge from The Cambridge Crystallographic Data Centre via www.ccdc.cam.ac.uk/data_request/cif. Correspondingly, its contribution was subtracted from the diffraction pattern by the Squeeze technique, using the PLATON software. [s1]

Table S1. Details of the X-ray data collection and structure refinements of compound **5**.

	5·DMSO
Formula	$C_6H_4N_{18}\cdot C_2H_6OS$
FW/ g mol^{-1}	406.4
Color	Orange
Habit	Prism
Crystal size /mm	0.08 × 0.134 × 0.307
Crystal system	triclinic
Space group	P-1
a/ Å	9.7539(16)
b/ Å	9.8451(17)
c/ Å	10.1270(18)
α/ °	79.433(6)
β/ °	61.224(6)
γ/ °	73.647(6)
V/ Å^3	816.6(2)
Z	2
$p_{calcd.}$/g·cm^{-3}	1.653
T /K	110 (2)
F (000)	416
μ/ mm^{-1}	0.249
Absorption correction	multi-scan
Dataset (h; k; l)	-11:11; -12:10; -12:12
θ range /°	2.298:25.345
Reflections collected	9080
Independent reflections	3090
$R_{int.}$	0.0235
Parameters	263
R1 [I>2σ(I)]	0.0455
WR2 [I>2σ(I)]	0.1244
R_1 (all data)	0.0535
wR2 (all data)	0.1303
Res. dens. /e·Å^{-3}	0.067
Solution	SHELXTL-2014
Refinement	SHELXL-2014/7

The first intramolecular hydrogen bond is toward the nitrogen atom N18 of the triazole that participates in an intramolecular hydrogen bond N18-H18···N12 with a D···A length of 2.818 Å and a D-H···A angle of 117° and the second is the nitrogen atom N8 of the amine that participates in an intramolecular hydrogen bond N8-H8B···N9 with a D···A length of 2.839 Å and a D-H···A angle of 123° (Table S1). The IR spectra of compound **5** were recorded and assigned using frequency analysis from an optimized structure.

Table S2. Hydrogen bonds present in the crystal structure of compound **5**

D-H···A	D-H/[Å]	H···A/[Å]	D···A/[Å]	D-H···A/[Deg.]
N18-H18···N12	0.880	2.304	2.818	**117.21**
N18-H18···O26	0.880	1.916	2.682	**144.69**
N8-H8B···N11	0.830	2.302	2.839	**122.77**
N8-H8A···N9	0.897	2.156	3.031	**164.96**
N16-H16···N21	**0.897**	**2.024**	**2.897**	**171.63**

DFT Calculation

Table S3a. Calculated isodesmic reactions and formation enthalpies (in kcal/mol and kJ/MOL) for reactions of formation of compounds **1**, **2**, **2B** and **2C**, from BPT and one or two equivalents of DAT (DMP = 3,5-dimethyl-1H-pyrazole).

	Starting Materials	Products	$\Delta_r H^\circ$ (kcal/mol)	$\Delta_r H^\circ$ (kJ/mol)
1	BPT + 1 Eq. DAT	Comp.**2B** + 1 Eq. DMP	-6.57	-27.49
2	BPT + 1 Eq. DAT	Comp. **2C** + 1 Eq. DMP	-9.16	-38.33
3	BPT + 2 Eq. DAT	Comp. **1** + 2 Eq. DMP	-17.14	-71.71
4	BPT + 2 Eq. DAT	Comp. **2** + 2 Eq. DMP	-14.76	-61.76

Table S3b. Computed formation enthalpies, kJ/mol at M06/6-31+g(2df,p) and CBS-4M level of theory. For solid phase correction, the following equation was used (according to the Trouton rule):

$\Delta_f H_{solidphase} = \Delta_f H_{gasphase} - 0.188 * T_{decomposition}$

	M06/6-31+g(2df,p)		CBS-4M			
	Gas phase, $\Delta_f H^\circ$ kJ/mol	Solid phase, $\Delta_f H^\circ$ kJ/mol	Gas phase, $\Delta_f H^\circ$ kJ/mol	Solid phase, $\Delta_f H^\circ$ kJ/mol	$T_{decomposition}$ °C	$T_{decomposition}$ K
1	820.96	702.50	806.04	687.57	357	630.15
2	830.95	720.76	827.66	717.46	313	586.15
3	840.19	721.91	828.91	710.63	356	629.15
4	1512.13	1425.06	1506.97	1419.89	190	463.15
5	1527.37	1440.29	1534.31	1447.24	190	463.15
6	1541.17	1454.85	1542.38	1456.06	186	459.15
7	859.39	754.64	846.03	741.29	284	557.15
8	905.12	800.76	897.00	792.63	282	555.15

Cytotoxicity Tests

In vitro biocompatibility study, based on the International Organization for Standardization 10993: Biological Evaluation of Medical Devices, Part 5: Tests for Cytotoxicity: in vitro Methods guidelines, was conducted on the compound to determine the potential for cytotoxicity. Normal Human Dermal Fibroblasts (NHDF) cells were propagated and maintained in cell culture dishes and seeded to wells containing single strength Modified Eagle's Medium supplemented with 10% serum and 1% antibiotics in a gaseous environment of 5 % CO_2. For this study, 0.33 cm^2 wells were seeded, labeled with passage number and date, and incubated at 37±1°C in 5 % CO_2 to obtain sub-confluent monolayers of cells prior to use. Aseptic procedures were used in the handling of the cell cultures. Eight repeats of culture wells were selected which contained a sub-confluent cell monolayer. The growth medium contained in the cultures was replaced with 100 µL media at 4 different concentrations of each test extract: 100%, 30%, 10%, 3%. Similarly, cultures were replaced with 100 µL of positive control (DMSO 10%, 3%, 1%, 0.3%) and 100 µL of the reagent control (DMEM) and 100 µL of negative control (Coverslips). The wells were incubated at 37±1°C in 5% CO_2 for 4±0.5 hours. Following incubation, the cultures were examined microscopically (10X) to evaluate cellular characteristics. The cultures were then prepared for an alamar-Blue assay by aspirating the media and then adding 10% alamar-Blue in culture media to the volume of cells. Viability/proliferation was determined by fluorimetric testing. Each culture well was evaluated for viability/proliferation by percent difference in metabolic activity from the reagent control, thus, allowing the determination of cytotoxicity of the tested articles.

Microtoxicity Tests

A microtoxicity assay was based on the International Organization for Standardization 11348-3. Determination of the Inhibitory Effect of Water Samples on the Light Emission of *Vibrio fischeri* (Luminescent bacteria test), was conducted to determine the EC_{50}, the effective concentration causing 50% inhibition of light output, of the compounds. The assay measures the reduction of luminescence of light emitting bacteria, *Vibrio fischeri*, due to exposure to materials. The BioTox kit (Aboatox Oy, Finland) was used for the determination of toxicity of aqueous samples. After 4±0.5 hrs of extraction, seven dilutions of different concentrations were prepared for the compounds as well as the control (blank) and the reference standard. All samples were placed in a 15 °C incubator. The bacteria were reconstituted in a diluent, and the reconstituted solution was placed in the 15 °C incubator for stabilization. Bacterial suspension (500 µL) was tested on the luminometer and immediately afterward, a sample (500 µL) was added to the bacteria, and the mixture was vortexed. The initial luminosity reading was recorded and the sample was returned to the 15 °C incubator. After 30 min, the luminosity was measured again, to determine the effect of the sample on the bacteria's luminescence. Each sample, control, and reference standard were tested for luminescence at 0 and 30 minutes to determine the EC_{50} of each test article. For the test to be valid, the reference substance (zinc sulfate) must cause 20% to 80% inhibition after 30 minutes. The correction factor calculated based on the blank results should range from 0.6-1.8.

Figures

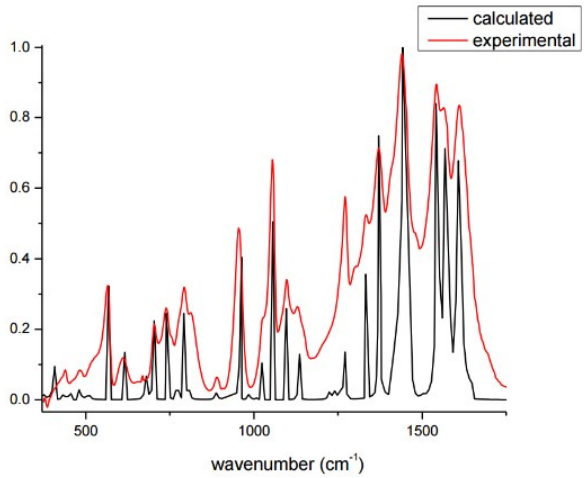

Figure S1. A comparison of the calculated FTIR spectrum with the measured spectrum of compound **5.**

The spectrum contains five major peaks at 1610, 1542, 1440, 1371 and 1097 cm^{-1} assigned 1650-1580 cm^{-1} as N-H primary amine, 1550-1450 cm^{-1} as N-H secondary amine, 1335-1250 cm^{-1} as C-N aromatic amine, 1250-1020 cm^{-1} as C-N stretching in the aliphatic amine, 1690-1640 cm^{-1} as the vibration of -C=N- bond.

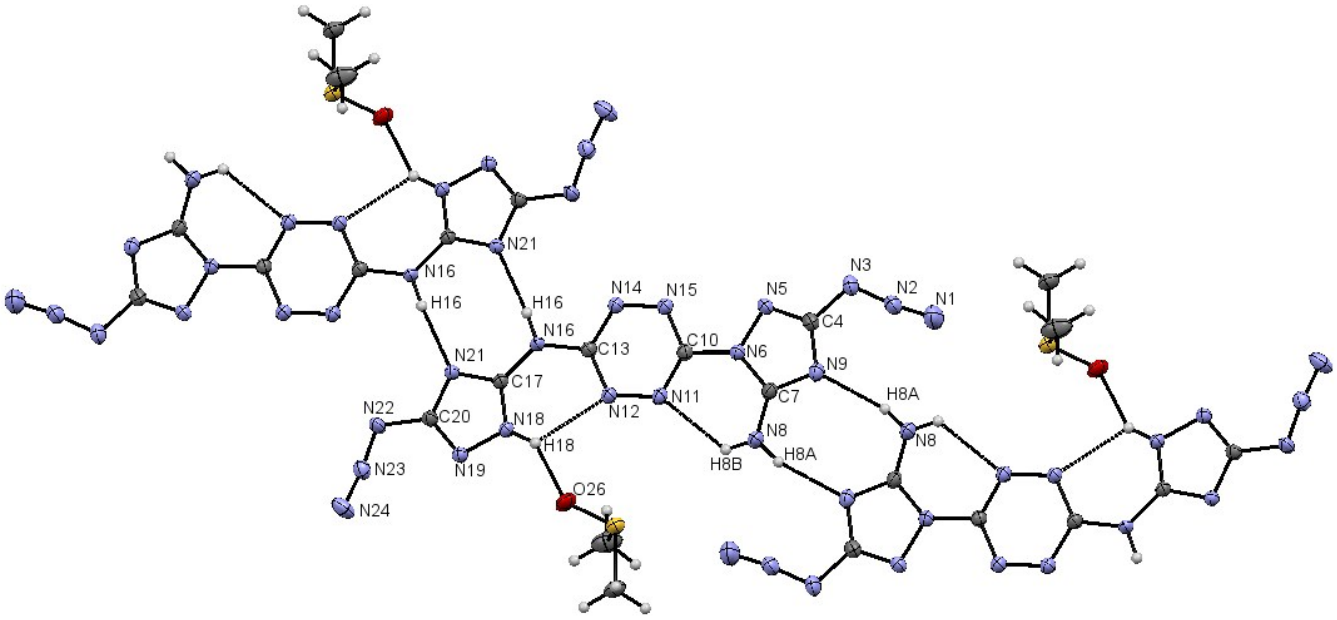

Figure S2. Interactions between compound **5** molecules in the unit cell and surrounding DMSO molecules.

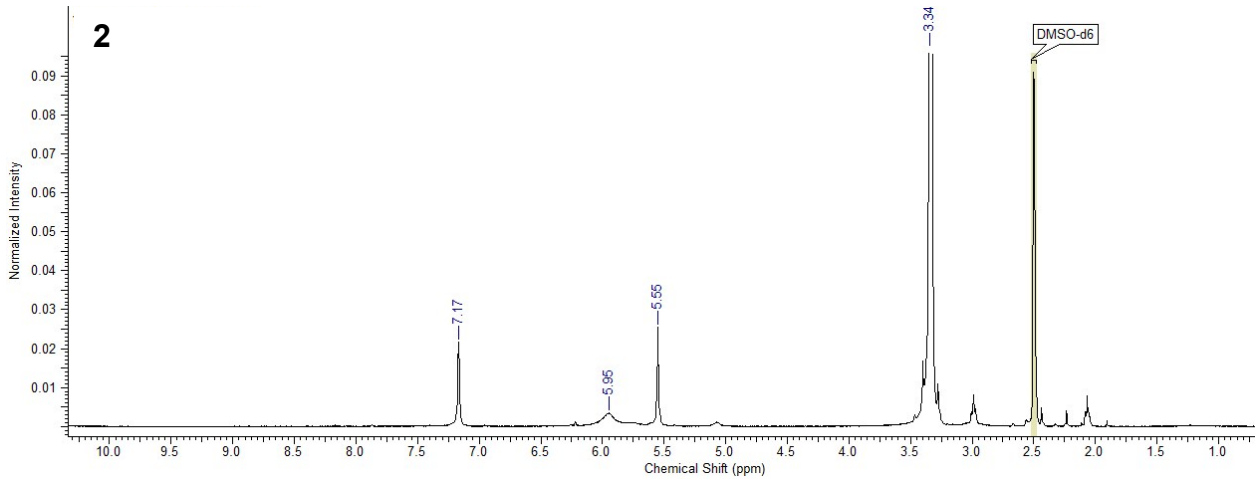
2
Normalized Intensity
Chemical Shift (ppm)
DMSO-d6
3.34
7.17
5.95
5.55

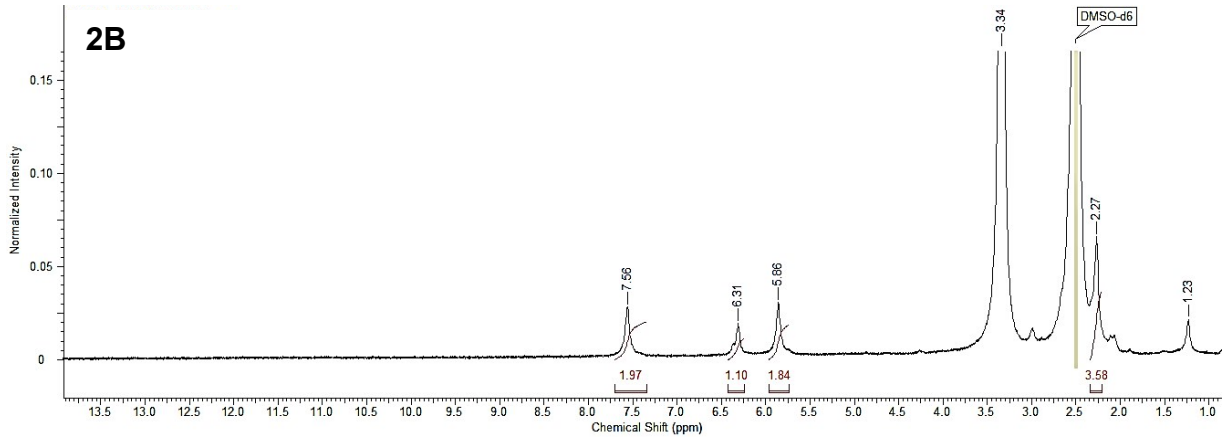
2B
Normalized Intensity
Chemical Shift (ppm)
DMSO-d6
3.34
7.56
6.31
5.86
2.27
1.23
1.97
1.10
1.84
3.58

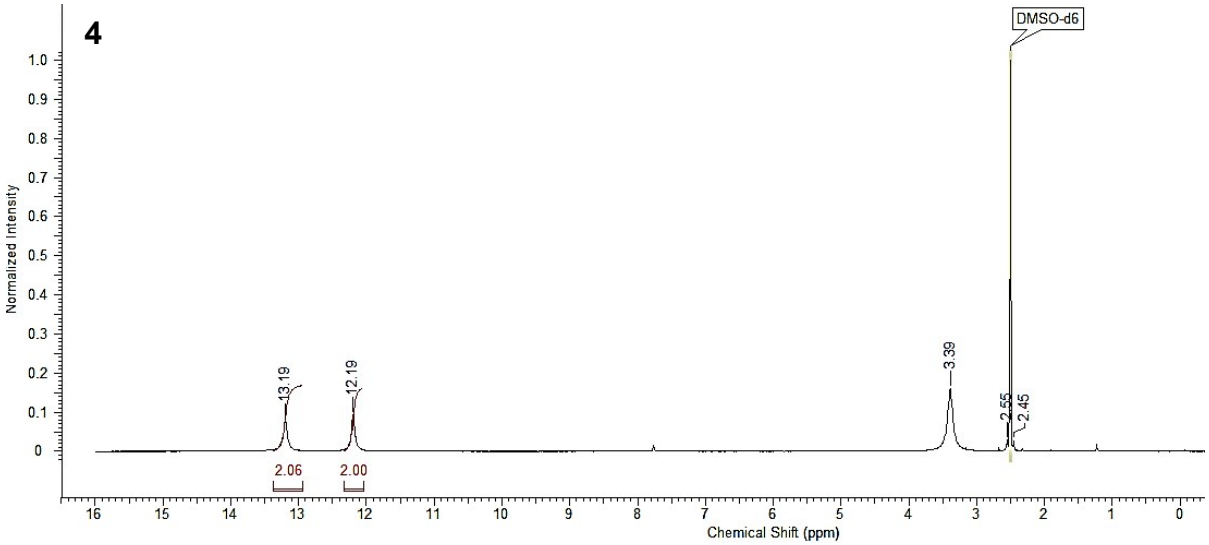
4
Normalized Intensity
Chemical Shift (ppm)
DMSO-d6
13.19
12.19
3.39
2.55
2.45
2.06
2.00

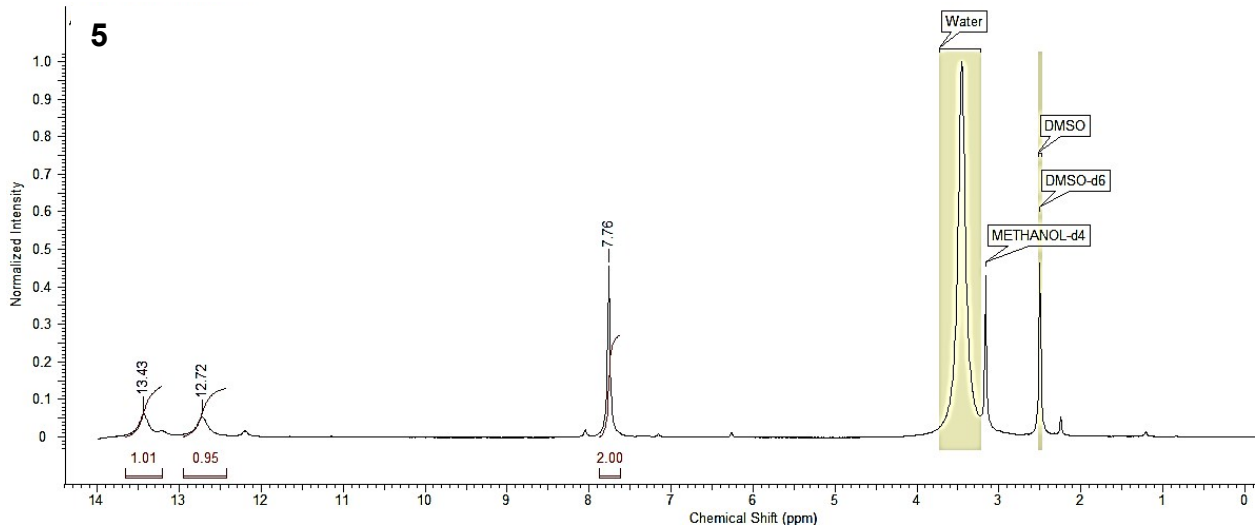
5
Water
DMSO
DMSO-d6
METHANOL-d4
7.76
13.43
12.72
1.01
0.95
2.00
Normalized Intensity
Chemical Shift (ppm)

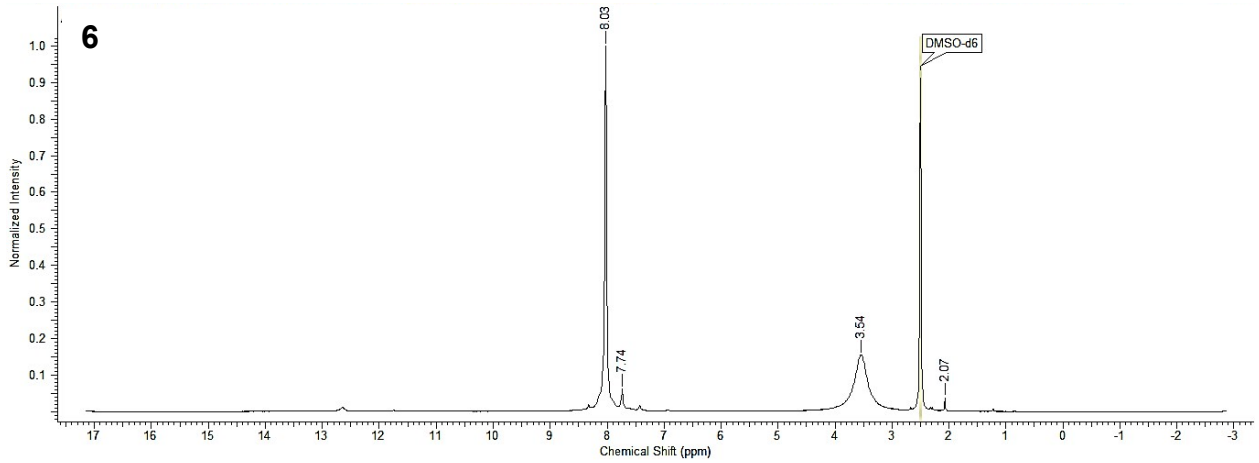
6
8.03
DMSO-d6
3.54
7.74
2.07
Normalized Intensity
Chemical Shift (ppm)

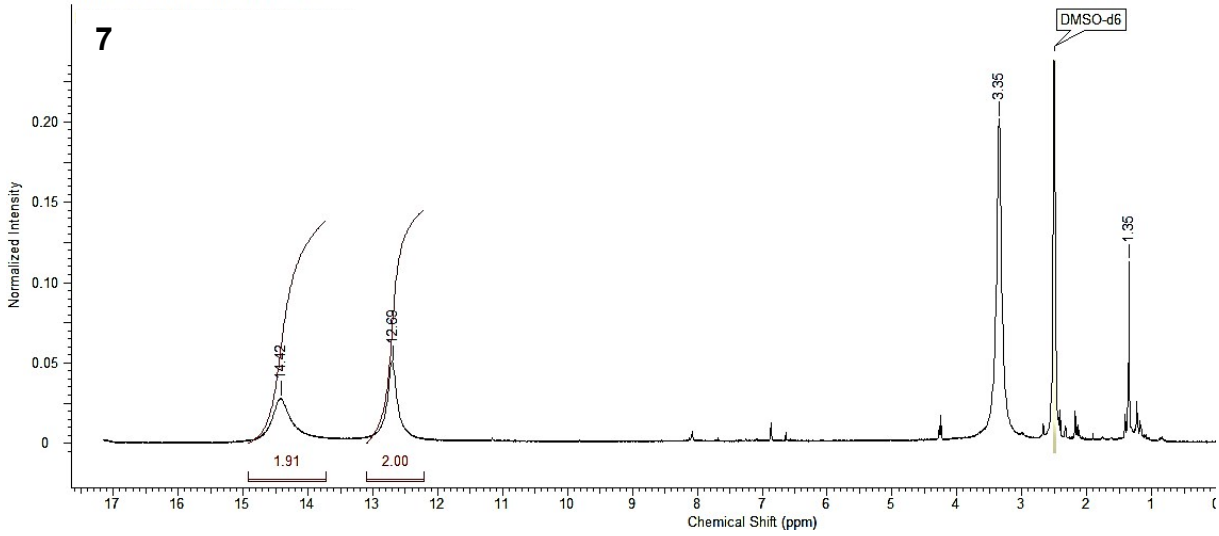
7
DMSO-d6
3.35
1.35
14.42
12.69
1.91
2.00
Normalized Intensity
Chemical Shift (ppm)

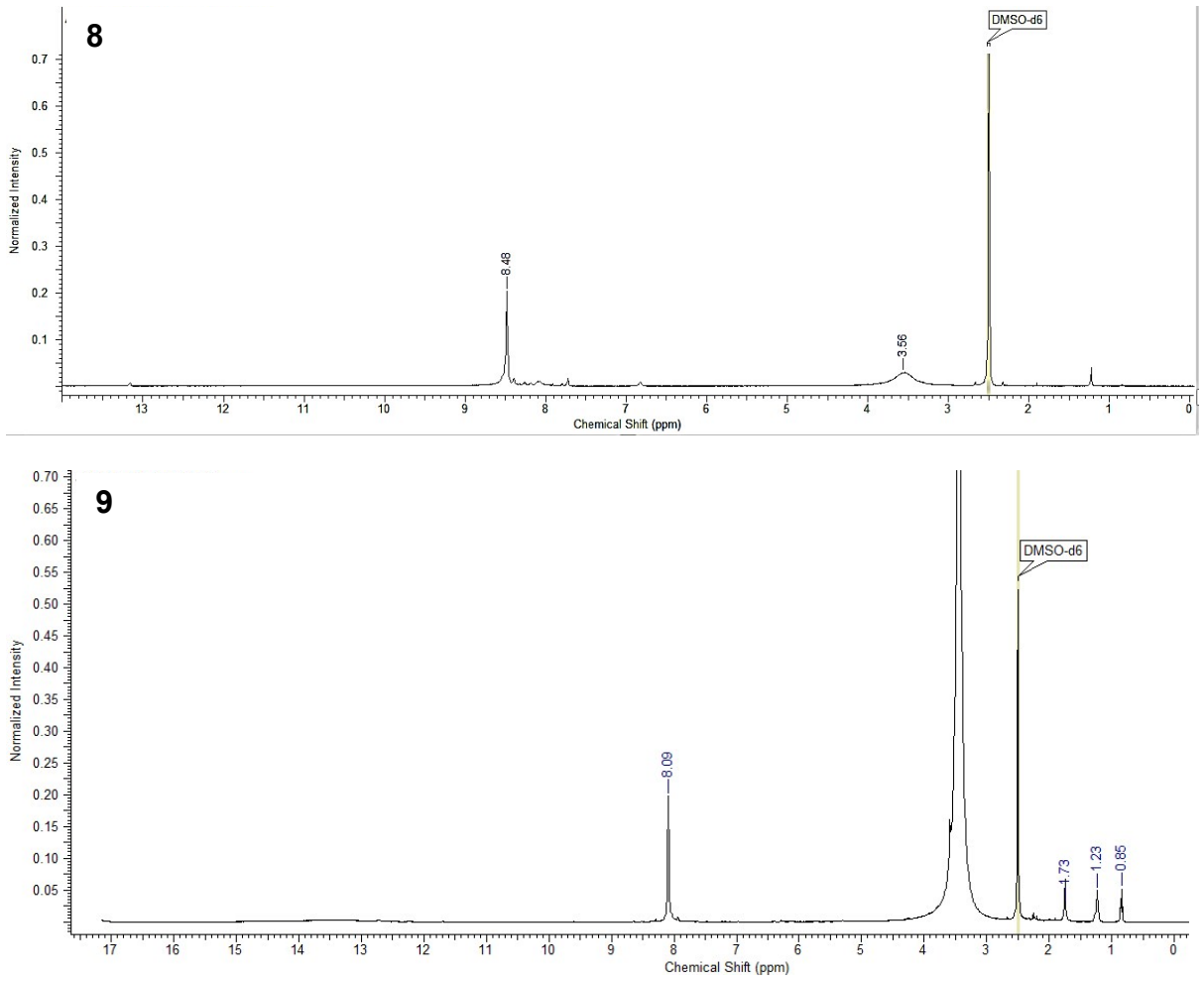

Figure S3. ^{1}H NMR of compounds **2, 2B, 4, 5, 6, 7, 8** and **9**.

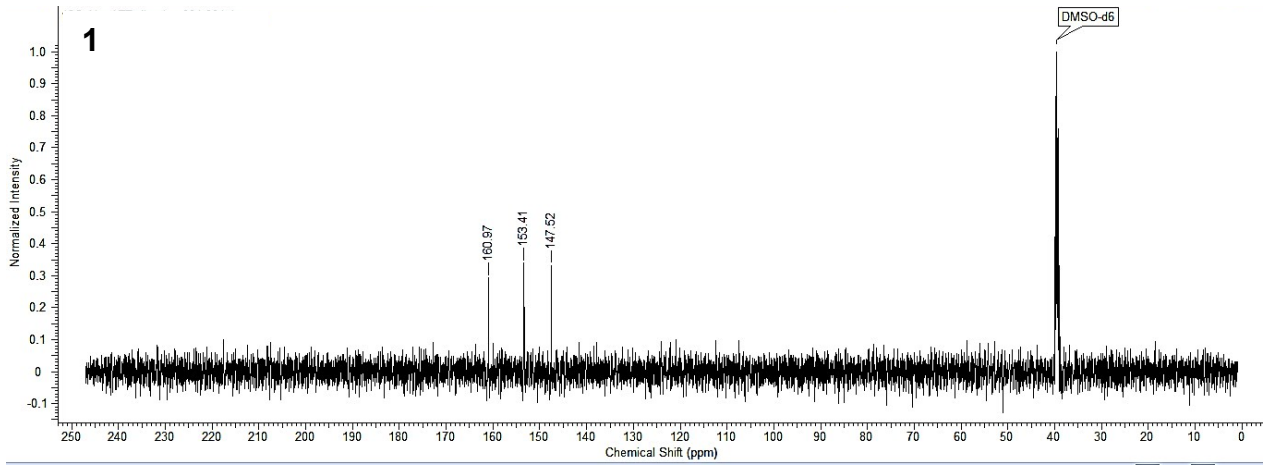

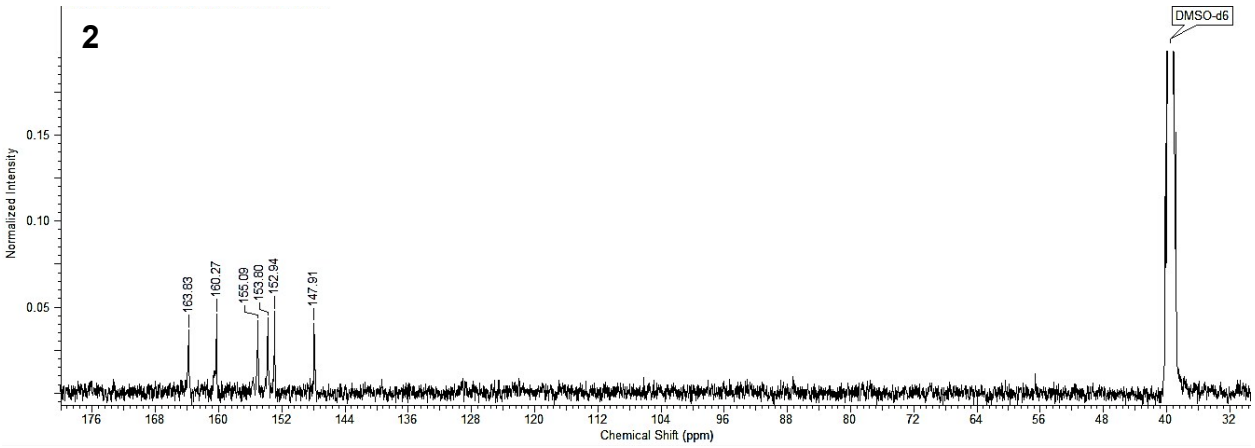
2
DMSO-d6
Normalized Intensity
0.15
0.10
0.05
163.83
160.27
155.09
153.80
152.94
147.91
176 168 160 152 144 136 128 120 112 104 96 88 80 72 64 56 48 40 32
Chemical Shift (ppm)

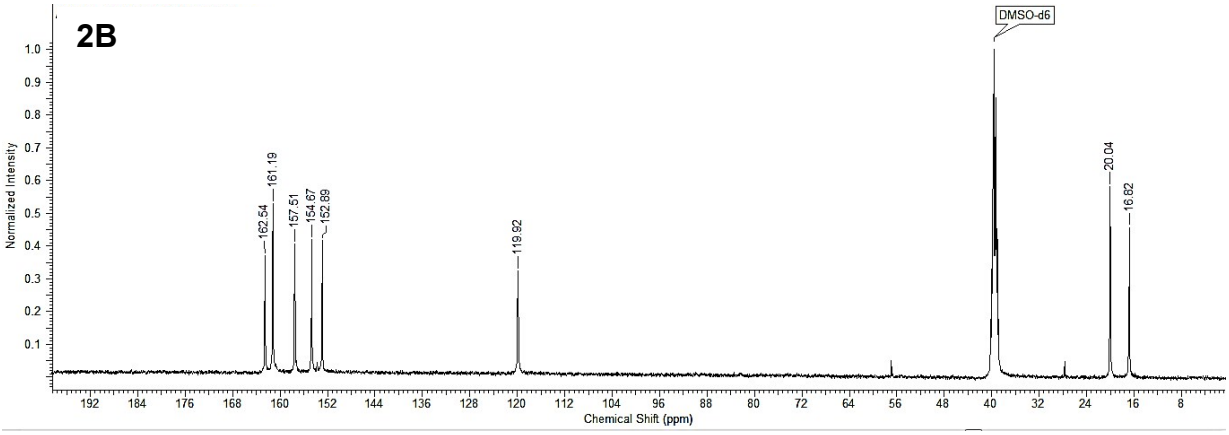
2B
DMSO-d6
Normalized Intensity
1.0
0.9
0.8
0.7
0.6
0.5
0.4
0.3
0.2
0.1
162.54
161.19
157.51
154.67
152.89
119.92
20.04
16.82
192 184 176 168 160 152 144 136 128 120 112 104 96 88 80 72 64 56 48 40 32 24 16 8
Chemical Shift (ppm)

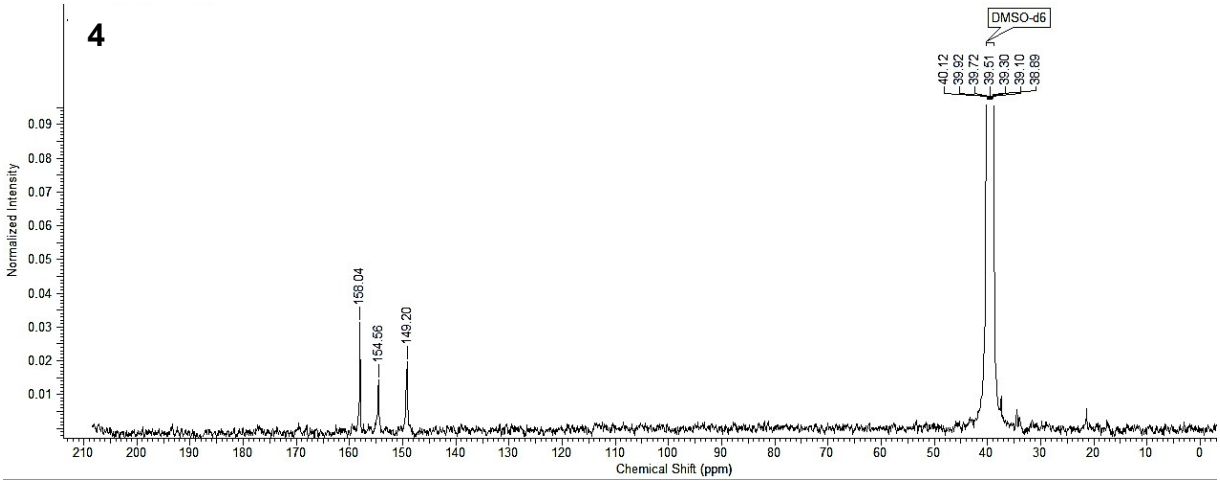
4
DMSO-d6
40.12
39.92
39.72
39.51
39.30
39.10
38.89
Normalized Intensity
0.09
0.08
0.07
0.06
0.05
0.04
0.03
0.02
0.01
158.04
154.56
149.20
210 200 190 180 170 160 150 140 130 120 110 100 90 80 70 60 50 40 30 20 10 0
Chemical Shift (ppm)

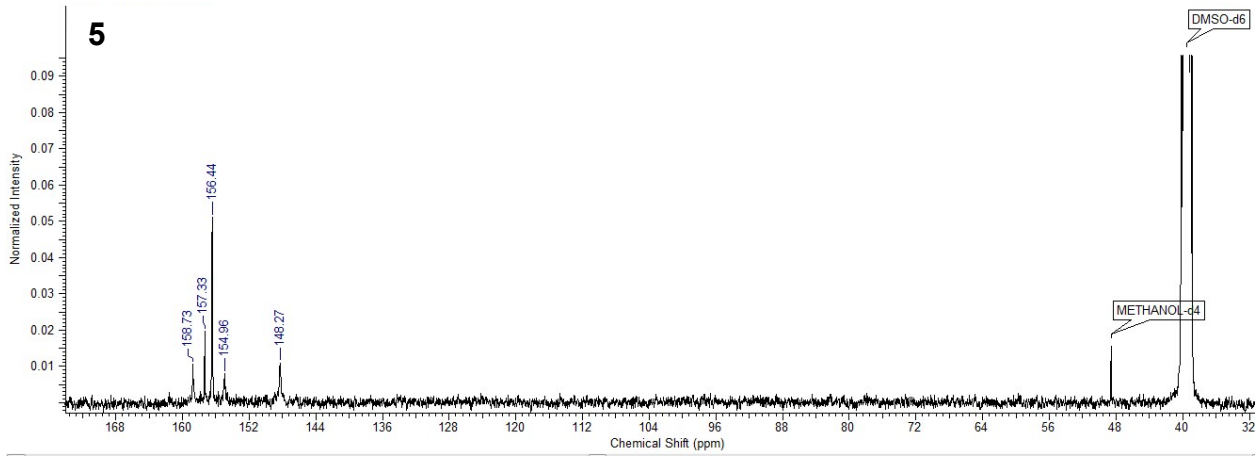
5
DMSO-d6
METHANOL-d4
158.73
157.33
156.44
154.96
148.27
Normalized Intensity
Chemical Shift (ppm)

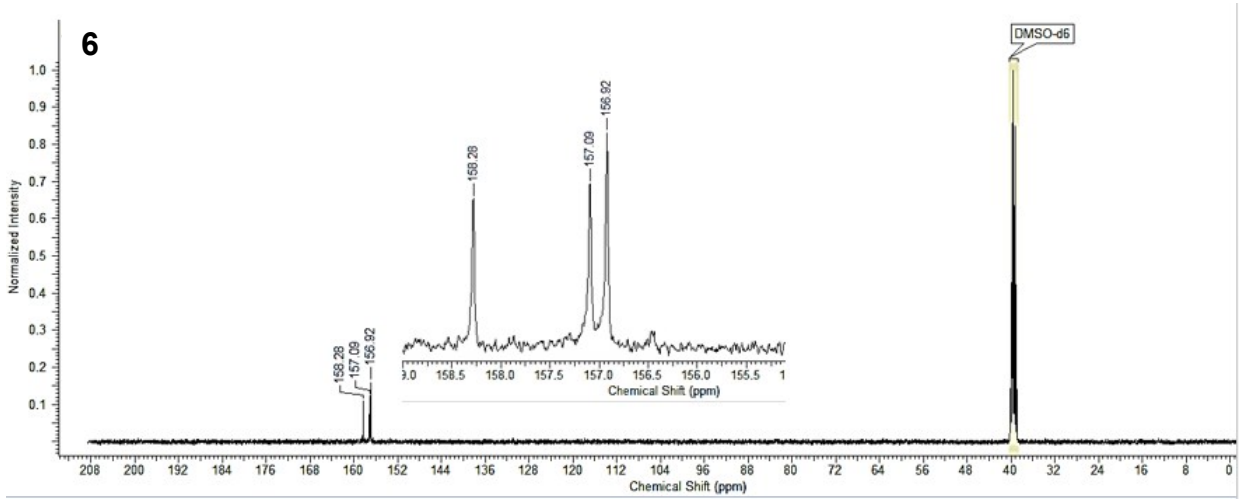
6
DMSO-d6
158.28
157.09
156.92
Normalized Intensity
Chemical Shift (ppm)

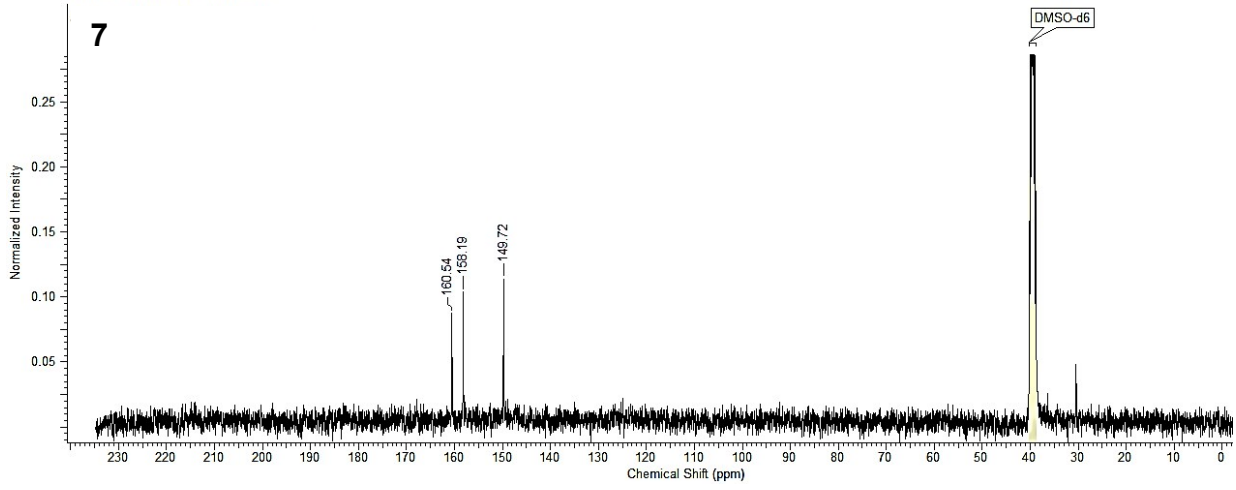
7
DMSO-d6
160.54
158.19
149.72
Normalized Intensity
Chemical Shift (ppm)

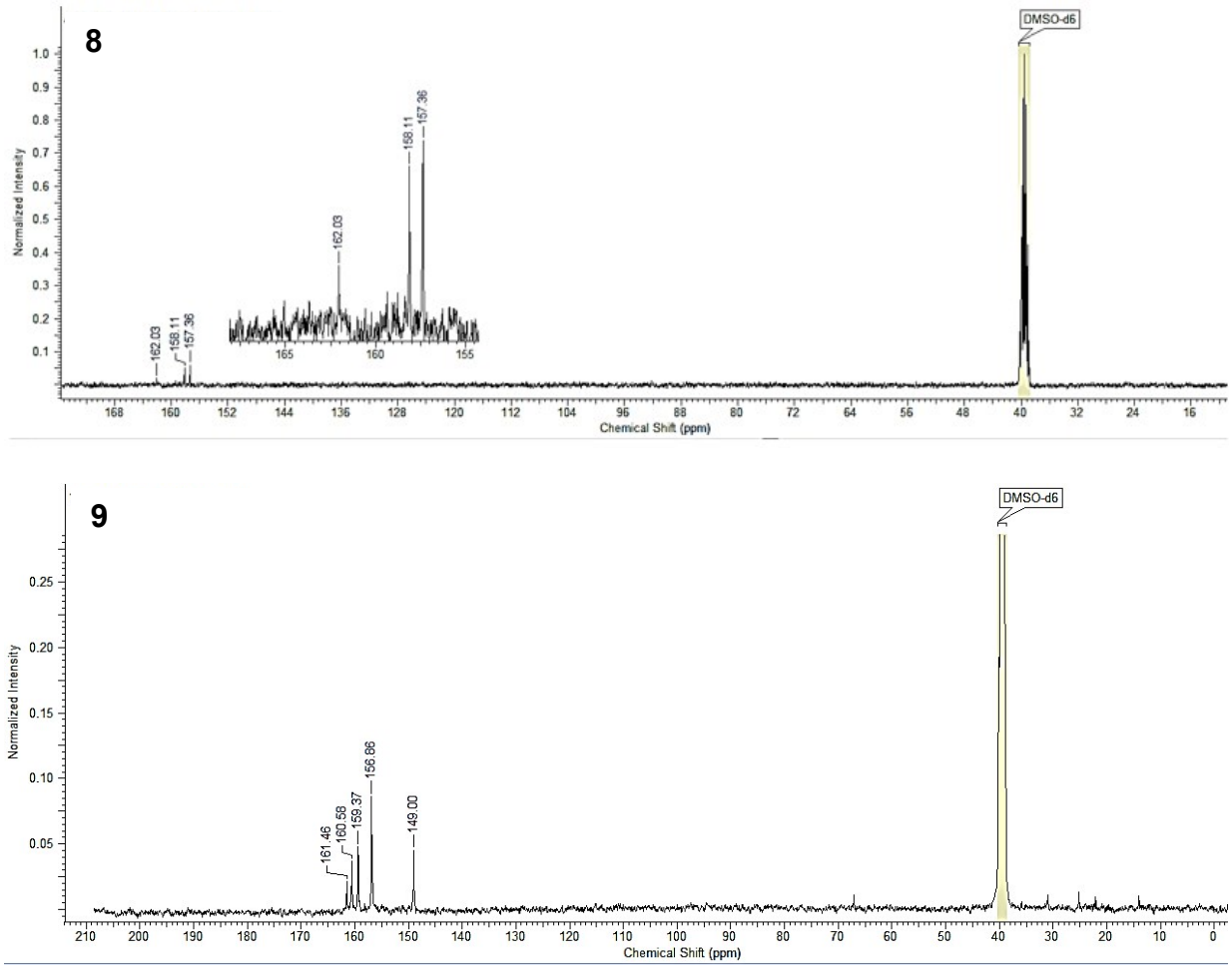

Figure S4. ^{13}C NMR of compounds **2, 2B** and **4-9**.

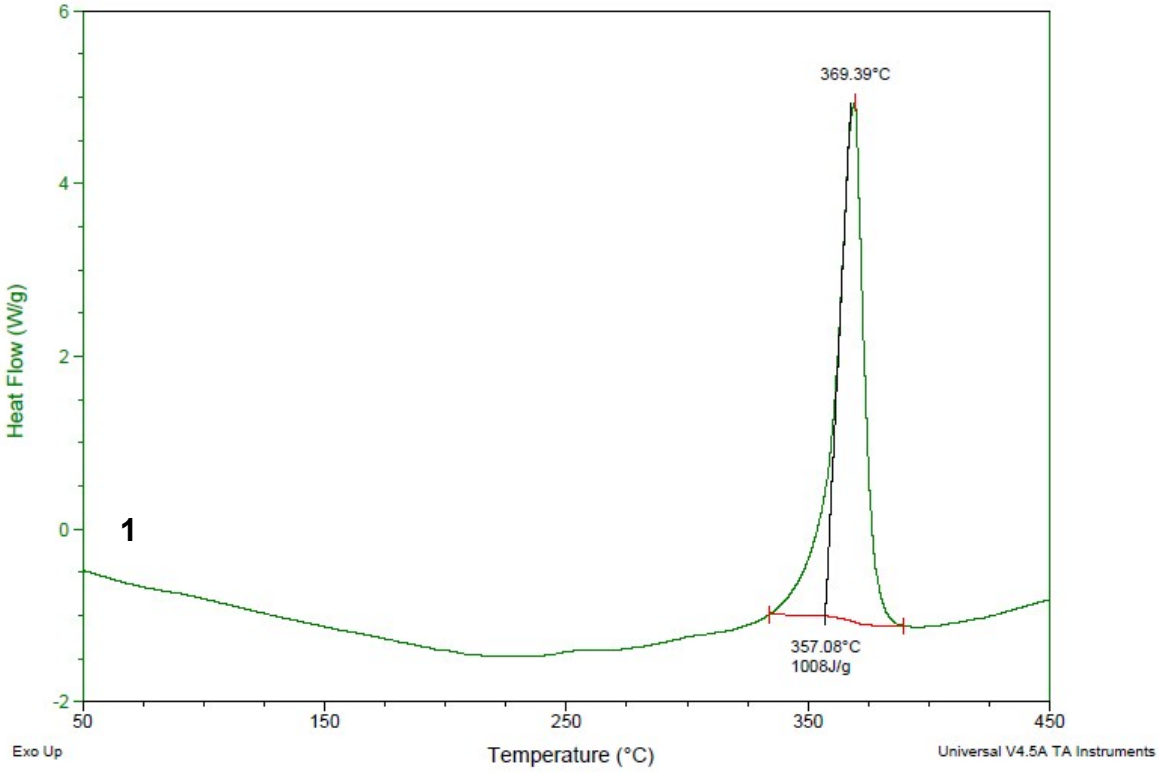
6
4
2
0
-2
Heat Flow (W/g)
1
369.39°C
357.08°C
1008J/g
50
150
250
350
450
Exo Up
Temperature (°C)
Universal V4.5A TA Instruments

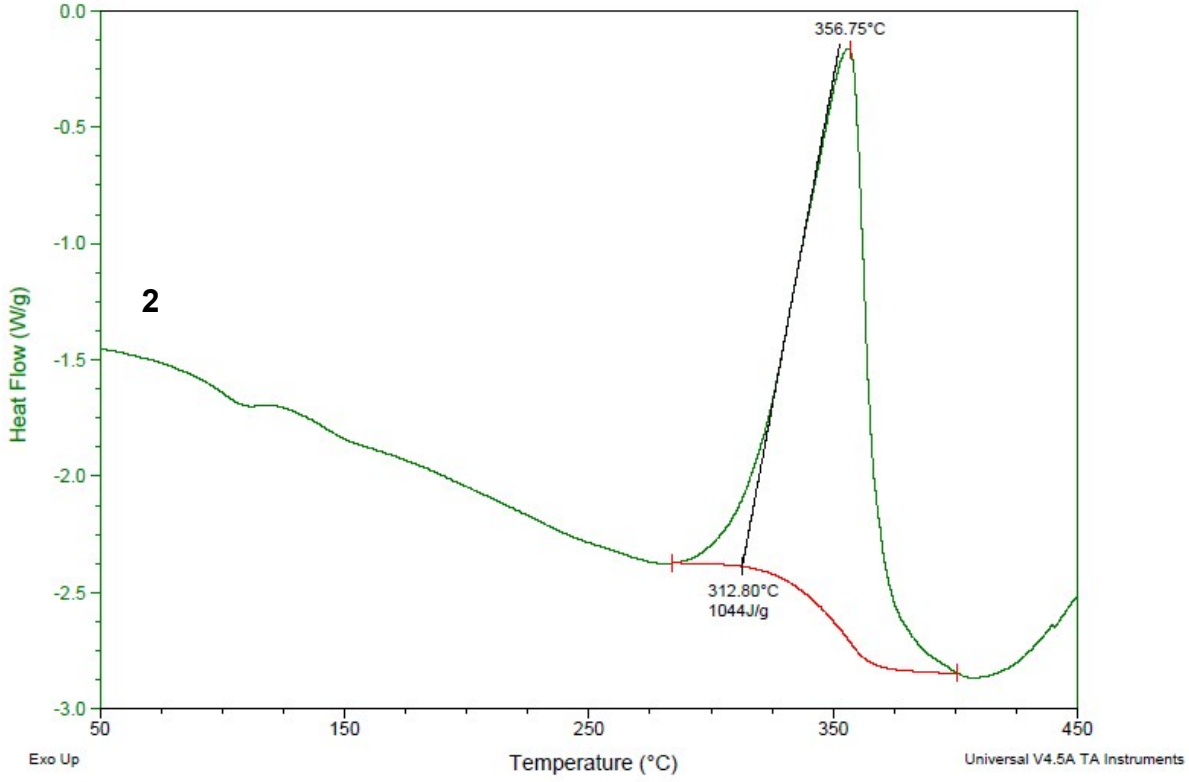
0.0
-0.5
-1.0
-1.5
-2.0
-2.5
-3.0
Heat Flow (W/g)
2
356.75°C
312.80°C
1044J/g
50
150
250
350
450
Exo Up
Temperature (°C)
Universal V4.5A TA Instruments

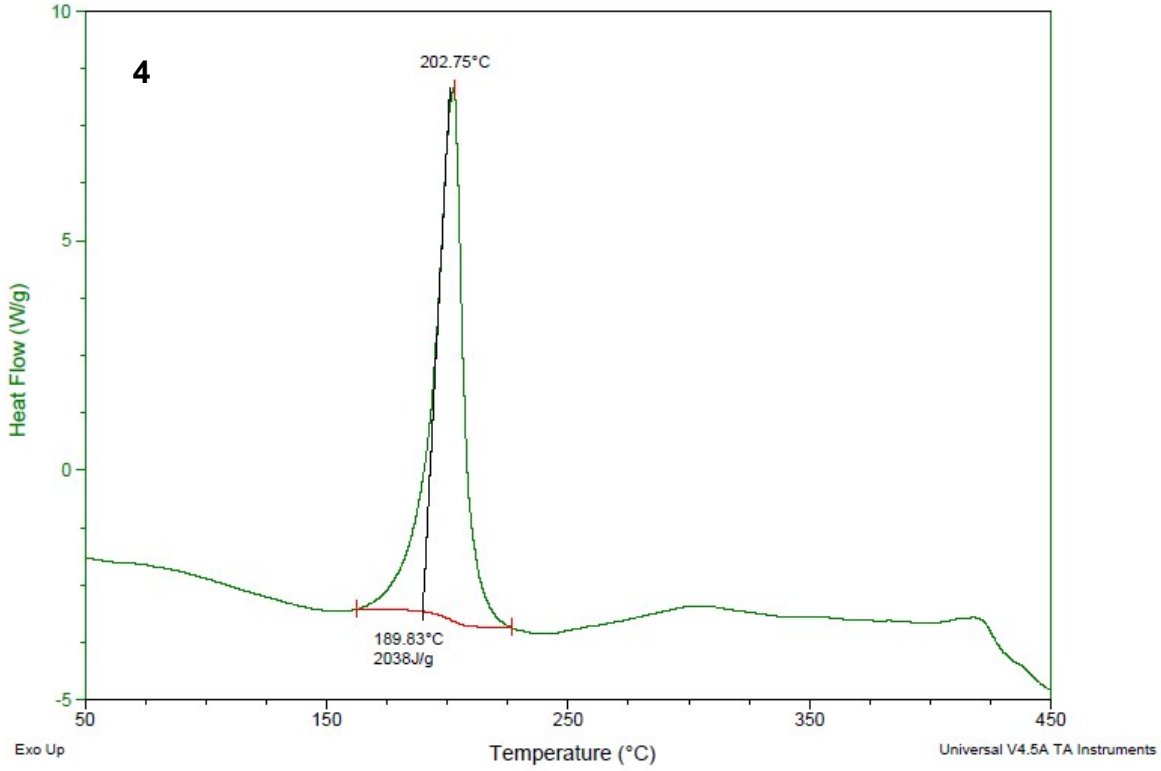
4
202.75°C
189.83°C
2038J/g
Heat Flow (W/g)
Temperature (°C)
Exo Up
Universal V4.5A TA Instruments

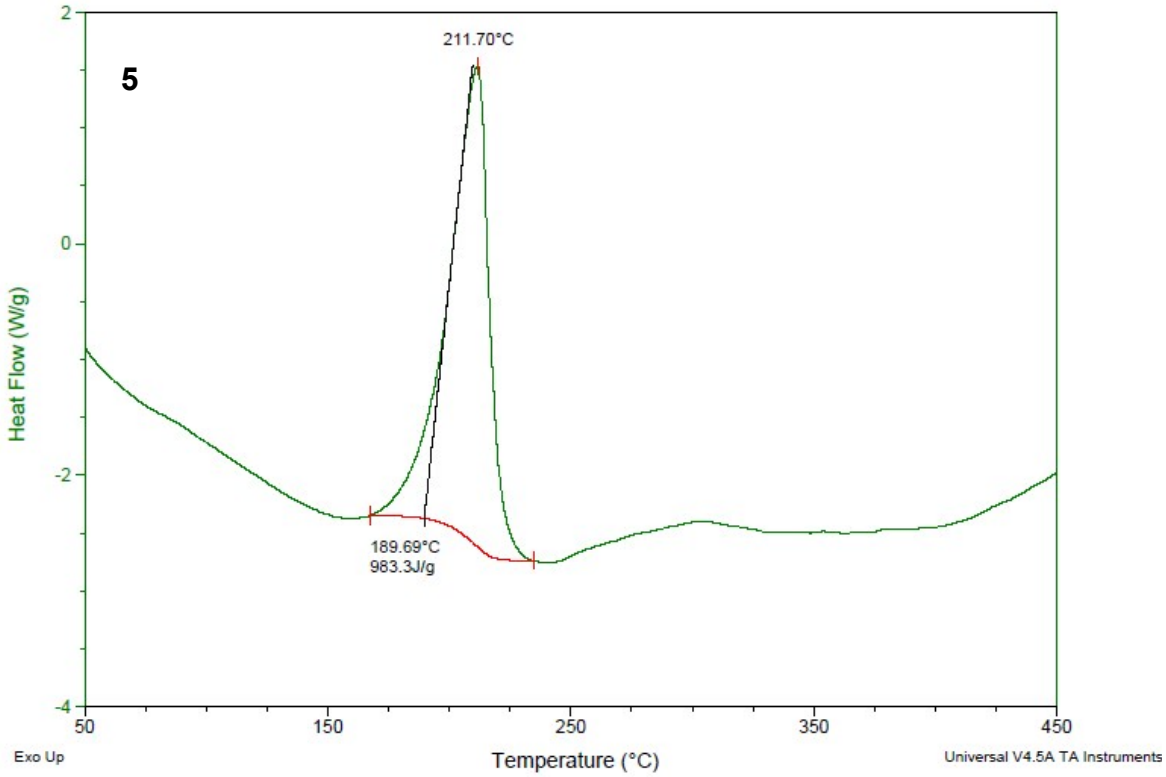
5
211.70°C
189.69°C
983.3J/g
Heat Flow (W/g)
Temperature (°C)
Exo Up
Universal V4.5A TA Instruments

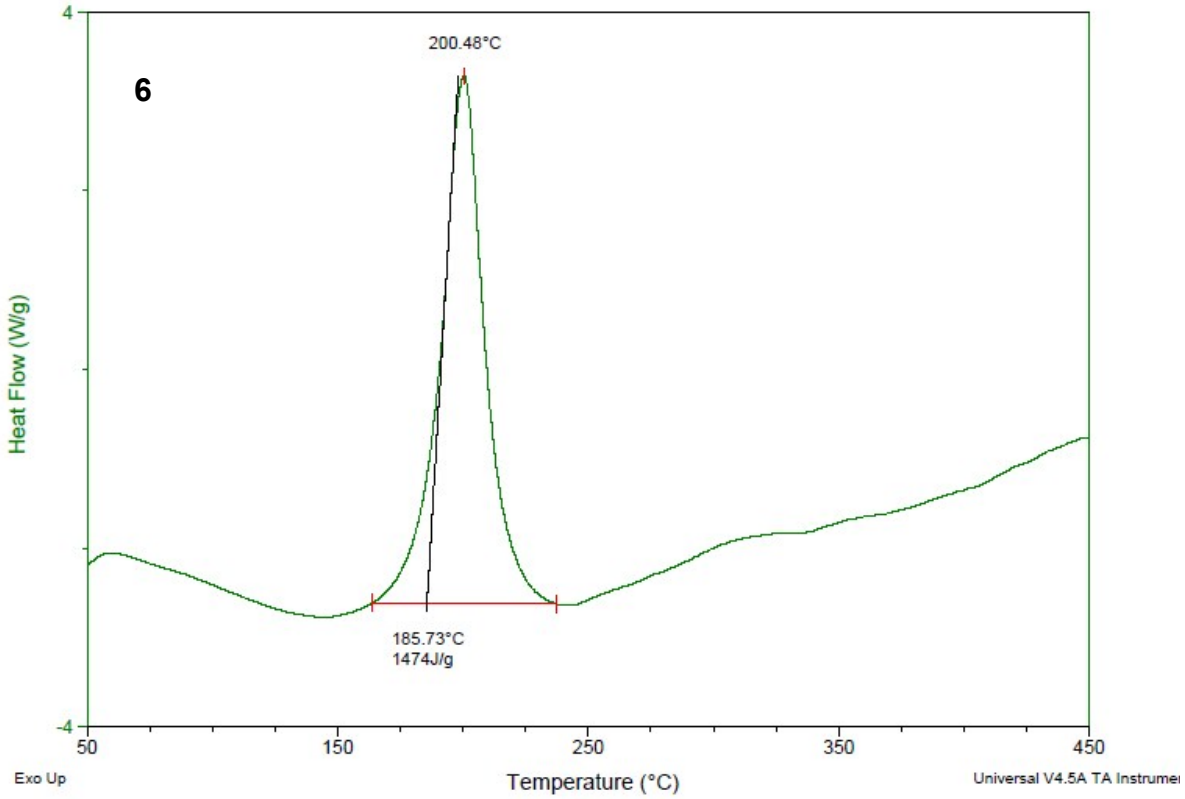
6
200.48°C
185.73°C
1474J/g
Heat Flow (W/g)
Temperature (°C)
Exo Up
Universal V4.5A TA Instrumer
4
-4
50
150
250
350
450

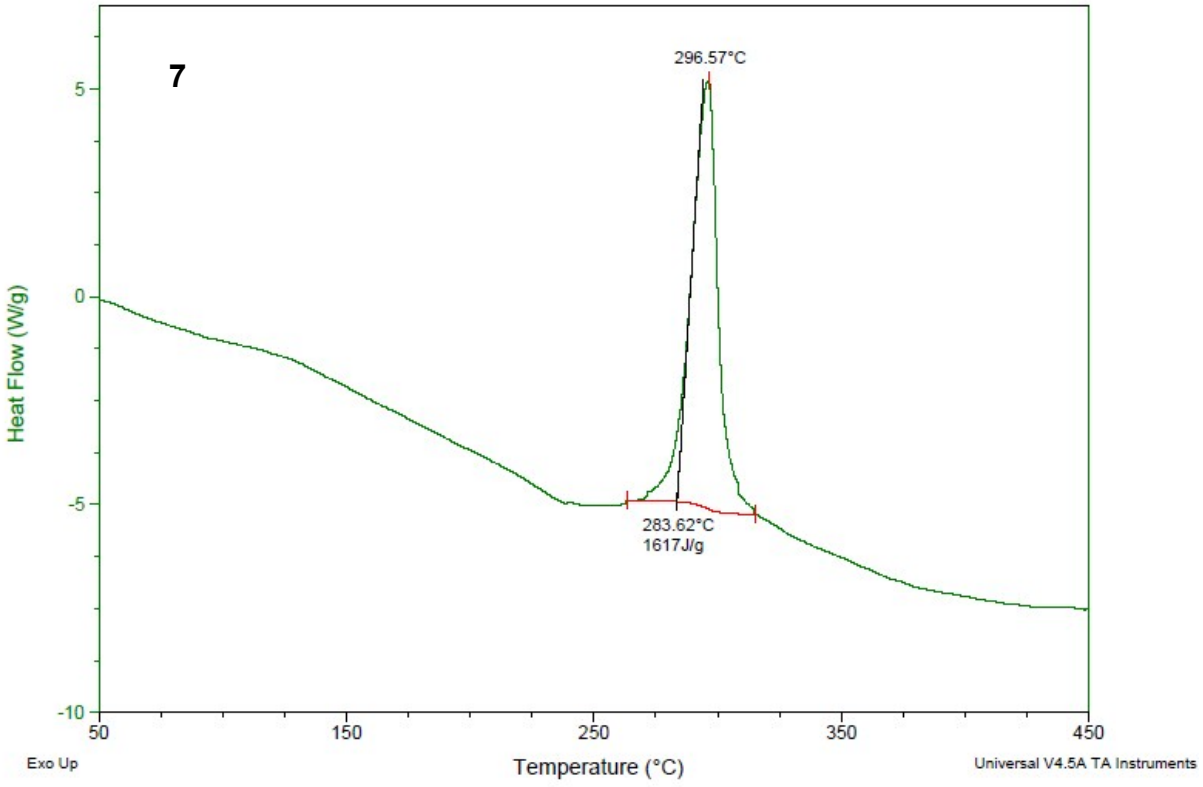
7
296.57°C
283.62°C
1617J/g
Heat Flow (W/g)
Temperature (°C)
Exo Up
Universal V4.5A TA Instruments
5
0
-5
-10
50
150
250
350
450

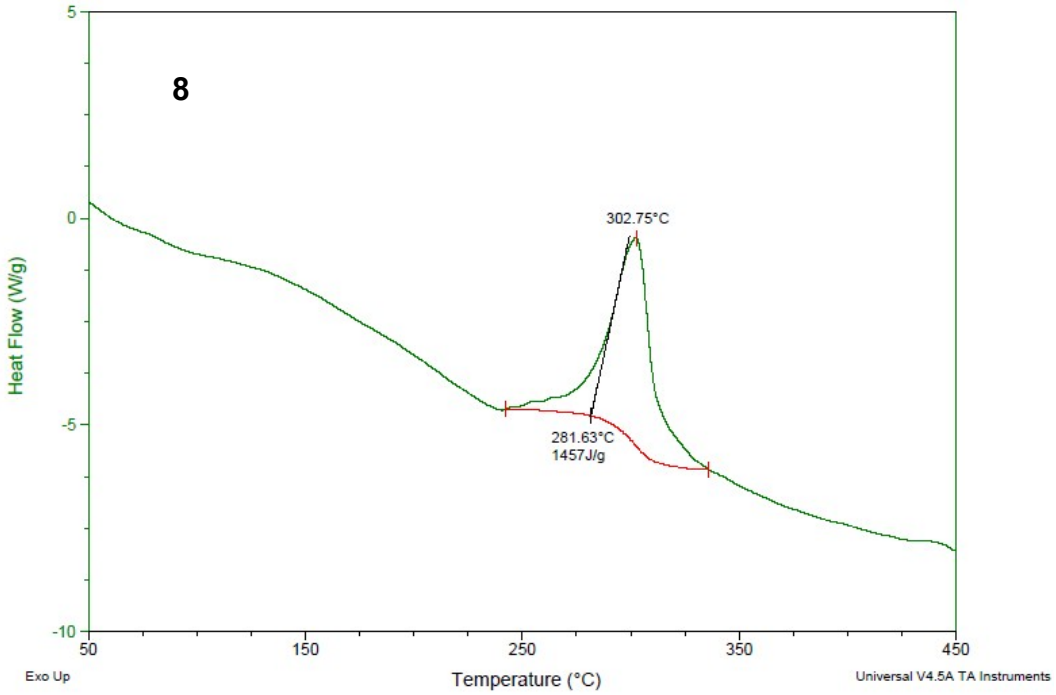

Figure S5. The DSC curves of compounds **1**, **2**, **4**, **5**, and **6**-**8**.

Table S4. Heat release measured by DSC for compound **1**, **2**, **4**, **5**, **6**, **7**, **8** and for reference RDX explosive.

	1	**2**	**4**	**5**	**6**	**7**	**8**	**RDX**
Δ_cH [*J/g*])	1088	1044	2038	983.3	1474	1617	1457	900

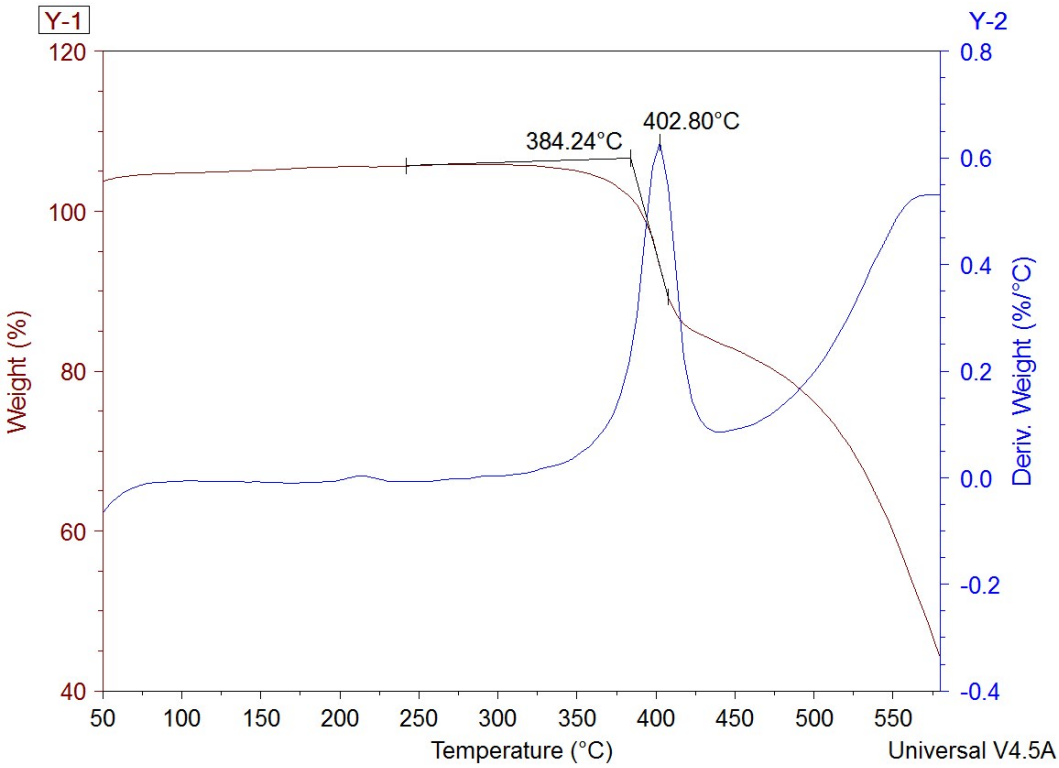

Figure S6. TG/DTG curves of **1**.

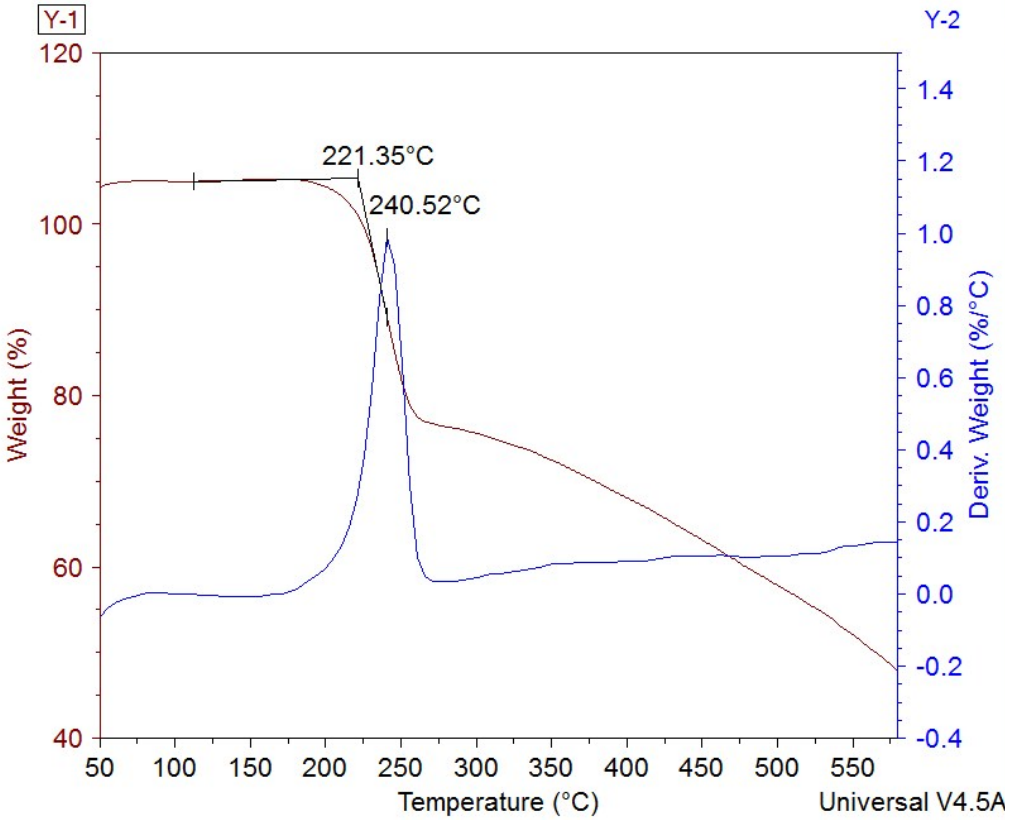

Figure S7. TG/DTG curves of **5.**

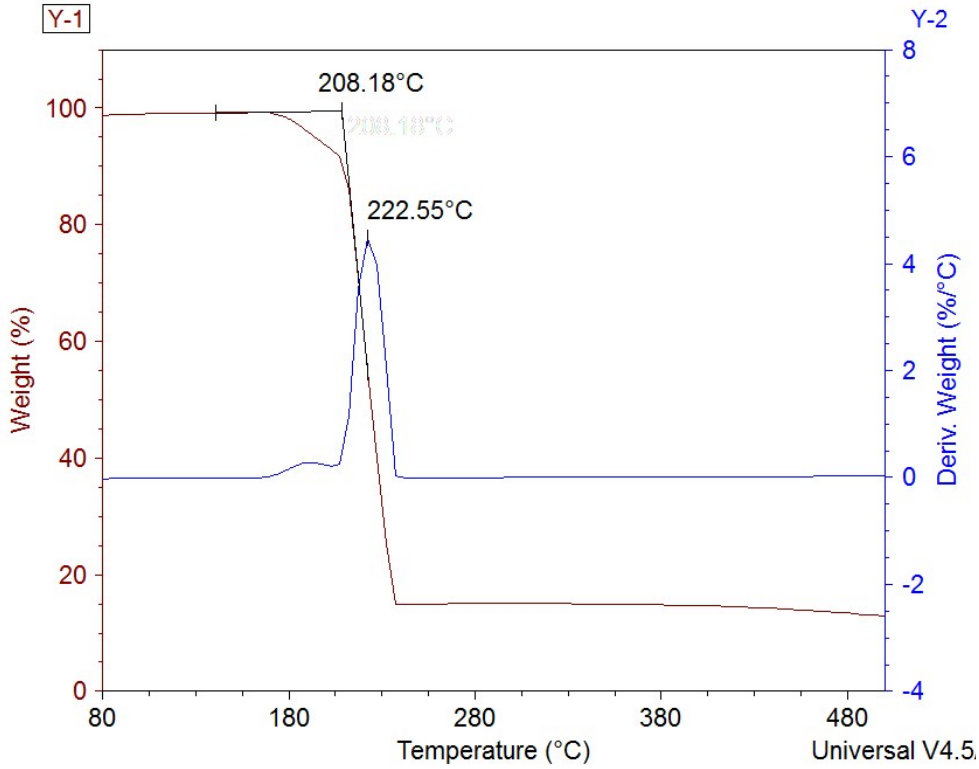

Figure S8. TG/DTG curves of **4.**

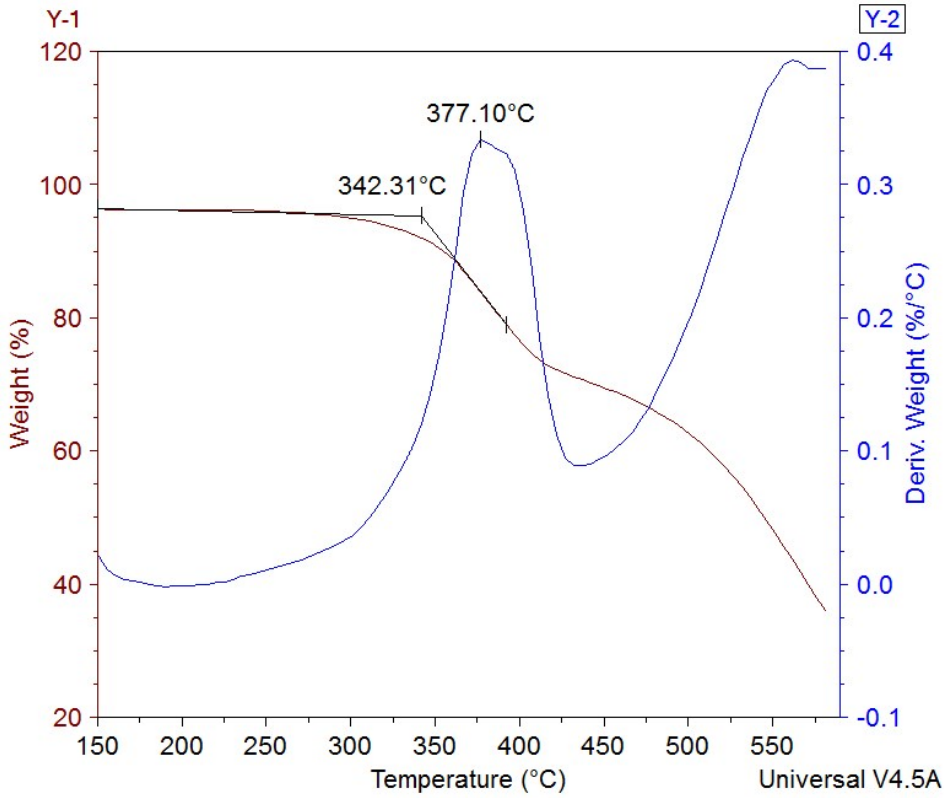

Figure S9. TG/DTG curves of **2.**

References

[s1] A.L. Spek, *Acta* Cryst. **2009**, *D65*, 148-155.

[s2]. M. J. Frisch, G. W. Trucks, H. B. Schlegel, G. E. Scuseria, M. A. Robb, J. R. Cheeseman, G. Scalmani, V. Barone, B. Mennucci, G. A. Petersson, H. Nakatsuji, M. Caricato, X. Li, H. P. Hratchian, A. F. Izmaylov, J. Bloino, G. Zheng, J. L. Sonnenberg, M. Hada, M. Ehara, K. Toyota, R. Fukuda, J. Hasegawa, M. Ishida, T. Nakajima, Y. Honda, O. Kitao, H. Nakai, T. Vreven, J. A. Montgomery, Jr., J. E. Peralta, F. Ogliaro, M. Bearpark, J. J. Heyd, E. Brothers, K. N. Kudin, V. N. Staroverov, T. Keith, R. Kobayashi, J. Normand, K. Raghavachari, A. Rendell, J. C. Burant, S. S. Iyengar, J. Tomasi, M. Cossi, N. Rega, J. M. Millam, M. Klene, J. E. Knox, J. B. Cross, V. Bakken, C. Adamo, J. Jaramillo, R. Gomperts, R. E. Stratmann, O. Yazyev, A. J. Austin, R. Cammi, C. Pomelli, J. W. Ochterski, R. L. Martin, K. Morokuma, V. G. Zakrzewski, G. A. Voth, P. Salvador, J. J. Dannenberg, S. Dapprich, A. D. Daniels, O. Farkas, J. B. Foresman, J. V. Ortiz, J. Cioslowski, and D. J. Fox, Gaussian 09 Revision C.01, Gaussian, Inc., Wallingford, CT, USA, 2010.

[s3] a) J. W. Ochterski, G. A. Petersson, J. A. Montgomery, J. Chem. Phys. 1996, 104, 2598–2619; b) J. A. Montgomery, M. J. Frisch, J. W. Ochterski, G. A. Petersson, J. Chem. Phys. 2000, 112, 6532–6542.

[s4] a) B. M. Rice, S. V. Pai, J. Hare, Combust. Flame 1999, 118, 445–458; b) B. M. Rice, J. J. Hare, J. Phys. Chem. A 2002, 106, 1770–1783; c) E. F. C. Byrd, B. M. Rice, J. Phys. Chem. A 2006, 110, 1005–1013.

[s5] a) P. J. Linstrom, W. G. Mallard (Editors), NIST Standard Reference Database Number 69, http://webbook.nist.gov/chemistry (accessed December 31, 2012); b) J. D. Cox, D. D. Wagman, V. A. Medvedev, CODATA Key Values for Thermodynamics, Hemisphere Publishing Corp., New York, 1984.

[s6] a) F. Trouton, Philos. Mag. 1884, 18, 54–57; b) M. S. Westwell, M. S. Searle, D. J. Wales, D. H. Williams, J. Am. Chem. Soc. 1995, 117, 5013–5015.